

# QSO spectra in cosmological tests

© S.A. Levshakov<sup>1,3</sup>, I.I. Agafonova<sup>1</sup> and P. Molaro<sup>2</sup>

<sup>1</sup>Ioffe Physico-Technical Institute, St.-Petersburg, Russia

<sup>2</sup>Osservatorio Astronomico di Trieste, Trieste, Italy

<sup>3</sup>Email: lev@astro.ioffe.rssi.ru

**Abstract:** A brief introduction to the current status of spectral observations of quasars is given in regard with two cosmological tests related to the nature of dark energy: the scaling law for the Cosmic Microwave Background temperature evolution with cosmological redshift  $z$ , and the variability of the fine-structure constant  $\alpha$ . New constraints on the modification of the linear behavior of  $T_{\text{CMB}}(z)$  as predicted by  $\Lambda$ -decaying models and on variations of  $\alpha$  are presented. Evolution of the spectral energy distribution of the metagalactic ultraviolet background radiation is also considered.

## 1. Introduction

Quasi-Stellar Objects (Quasars, QSOs), as the most powerful objects in the Universe, are unique point-like background sources suitable to probe the physical state and the chemical composition of the intergalactic medium (IGM) in a wide interval of redshifts from  $z=0$  (the present epoch) up to  $z \approx 7$  (97% of the total age of the Universe). The QSO continuum spectrum from the optical to hard X-rays emerges from physical scales ranging from AU to parsec, and the QSO bolometric luminosities are as high as  $10^{47}$  erg/s. The most prominent features in quasar spectra are broad emission lines from resonant ultraviolet transitions of HI, NV, OVI, CIV, SiIV, and MgII [1]. There are also numerous narrow absorption features in the spectral range shortward the emission HI Ly- $\alpha$  line (so called Ly- $\alpha$  forest). The majority of these lines arise in the intergalactic gas clouds at different cosmological redshifts. Some of them belong to the extended halos of the intervening galaxies. The density of the Ly- $\alpha$  forest lines increases with increasing redshift, and at  $z > 5$  the quasar continuum shortward the emission HI Ly- $\alpha$  line is almost completely blocked by the forest lines. It is suggested that at  $z = 5-6$  we observe the final stage of the hydrogen reionization [2]. Along with a rich hydrogen absorption line spectrum, the IGM presents metal absorptions (all elements with atomic numbers  $Z > 2$ ) arising in discrete intergalactic clouds. Metal absorption systems detected in QSO spectra can be roughly classified into three groups: (1) highly photoionized Ly- $\alpha$  forest absorbers with  $10^{12} \text{ cm}^{-2} \leq N(\text{HI}) \leq 10^{17} \text{ cm}^{-2}$  and metal absorption in CIII, SiIII, CIV, SiIV, NV, OVI; (2) Lyman Limit Systems (LLSs) with  $10^{17} \text{ cm}^{-2} \leq N(\text{HI}) \leq 10^{19} \text{ cm}^{-2}$  and absorption features due to the same highly ionized atoms as well as their lower ionization counterparts such as CII, SiII, and MgII, AlII, FeII; and (3) Damped Ly- $\alpha$  Absorbers (DLAs) with  $10^{19} \text{ cm}^{-2} < N(\text{HI}) < 10^{22} \text{ cm}^{-2}$  and the same set of ions augmented with neutral atoms CI, OI, NI, SI, FeI [3,4] and sometimes (seldom) molecular hydrogen  $\text{H}_2$  transitions of the Lyman and Werner UV bands [5,6]. A comprehensive review of the physical characteristics of the IGM is given in [7].

## 2. Extragalactic Cosmic Microwave Background Temperature

Spectral observations of extrasolar and extragalactic sources permit to analyze the Cosmic Microwave Background (CMB) radiation temperature locally (at redshift  $z = 0$ ) as a function of the spatial coordinate and in earlier cosmological epoch ( $z > 0$ ) as a function of the spatial and cosmic time (redshift) coordinates. The dependence  $T(z)$  may not be unique but determined by a particular cosmological model. For instance, a linearly evolving CMB temperature,  $T(z) = T(0)(1+z)$ , is predicted within the framework of the standard cold dark matter model with a cosmological constant  $\Lambda$  ( $\Lambda$ CDM). Along with the  $\Lambda$ CDM model, other cosmological scenarios are widely discussed in the literature with respect to mechanisms responsible for the late time acceleration of the Universe [8]. This acceleration is usually attributed to a dark energy component with negative pressure which can induce repulsive gravity. The existence of dark energy is supported by observations of type Ia supernovae [9] and by the results of Wilkinson microwave anisotropy probe (WMAP)

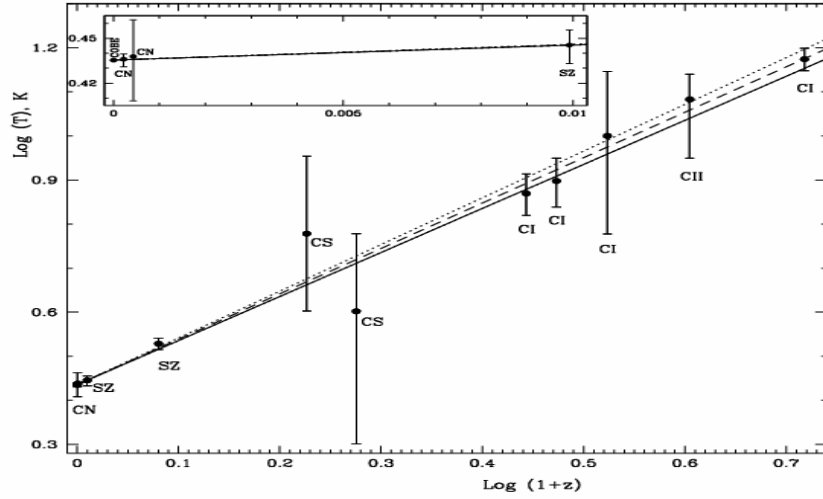


Fig. 1 Evolution of the radiation temperature  $T$  as a function of redshift  $z$ . Observations are shown by dots with  $1\sigma$  error bars (see text for details). The solid line is the  $(1+z)$  scaling law as predicted in the standard  $\Lambda$ CDM model. The dashed line shows the best fit to the alternative power law type scaling  $T \propto (1+z)^{1-\beta}$  with  $\beta = -0.03$ . The dotted lines are the  $\pm 0.03$  ( $1\sigma$ ) boundaries of  $\beta$ . The insert represents a magnified view of the region  $z \leq 0.0231$  (the redshift of the Coma cluster).

observations [10]. The most natural candidate for dark energy is the cosmological constant  $\Lambda$  which can be interpreted as vacuum energy [11,12]. However, the assumption that the dark energy is equivalent to  $\Lambda$  leads to a so called *cosmological constant problem* [11]: the observed value of  $\Lambda$  is too small, of about 120 orders of magnitude smaller than the vacuum energy that created the inflation epoch. To solve this problem, it was suggested that  $\Lambda$  decreases in course of cosmic time from a large value at the Planck time to its present quantity. In this process, any decrease of the energy density of the vacuum is to be balanced by a corresponding increase elsewhere to keep hold of energy conservation. A decaying vacuum that converts its energy into radiation is one of a possibility. The extra photons produced by a vacuum decay are thermalized due to Compton and bremsstrahlung processes [13-15]. Decaying  $\Lambda$  cosmologies have been considered in different contexts. An important issue for us is a predicted thermal evolution giving rise to a specific CMB temperature-redshift dependence. An example of such a modified relation is given in [16]:  $T(z) = T(0)(1+z)^{1-\beta}$ , where  $0 \leq \beta \leq 1$ , i.e. these  $\Lambda$  decaying models predict a lower temperature at high redshift as compared with the  $\Lambda$ CDM value. Another class of models with a variable cosmological term  $\Omega_\Lambda$  which is a function of the scale factor  $a$ ,  $\Omega_\Lambda = \Omega_{\Lambda,1} + \Omega_{\Lambda,2} a^{-m}$ , have been considered in [13] and in references cited therein. In order to validate standard or non-standard cosmological models for the functional scaling of the background radiation temperature, there were suggested different observational tests. The current status of these observations is considered below.

The most accurate value of the local CMB temperature measured by the *COBE* experiment is  $T(0) = 2.725 \pm 0.001$  K [17]. The corresponding relative error equals  $\delta \approx 0.04\%$ . Additional local but extrasolar values of the background radiation temperature were estimated from observations of interstellar molecular clouds. Namely, the relative strengths of the low rotational level transitions of cyanogen (CN) at  $\lambda 3874.0$  E  $R(1)$  and  $\lambda 3874.6$  E  $R(0)$  measured toward several Galactic stars yield the excitation temperature  $T_{01} = 2.729(+0.023, -0.031)$  K [18] with an accuracy of  $\delta \approx 1\%$ . Similarly, the excitation temperature of the cyanogen molecule was recently derived from the CN observations beyond the Milky Way in the Magellanic Clouds,  $T_{01} = 2.74(+0.16, -0.18)$  K [19], so  $\delta \approx 6\%$ . These extrasolar and extragalactic values are in good agreement with the *COBE* estimation. Thus, cosmological models predicting at  $z = 0$  non-Planckian spectra of the background radiation can be ruled out if they deviate by more than 1% (or 6% in case of the Magellanic Clouds constraint) from the blackbody spectrum. However, local observations do not allow to distinguish between the standard model and cosmological models with a blackbody spectrum but different  $T(z)$  dependences.

At low redshifts ( $0 < z < 1$ ), the functional scaling of the CMB temperature can be estimated from measurements of the Sunyaev-Zel'dovich (SZ) effect in the direction to clusters of galaxies. Relatively

simple spectral behavior and the independence on redshift in the  $\Lambda$ CDM model make the SZ observations a sensitive tool for the absolute CMB temperature measurements at the redshift of the clusters of galaxies. Using data of the Coma cluster (A1656,  $z = 0.0231$ ) and A2163 ( $z = 0.203$ ) over four bands at radio and microwave frequencies the following radiation temperatures have been obtained [20,21]:  $T_{A1656} = 2.789(+0.080, -0.065)$  K, and  $T_{A2163} = 3.377(+0.101, -0.102)$  K. For both measurements the error is  $\delta \approx 3\%$ . The values expected for the standard model equal to  $2.788 \pm 0.001$  K and  $3.278 \pm 0.001$  K, correspondingly. Thus, the first SZ estimates are in agreement with the linear dependence  $T$  on  $z$  within the 3% uncertainty interval in the redshift range  $0 < z \leq 0.2$ . The possibility to constrain the cosmological behaviour of  $T(z)$  at higher redshifts from multifrequency SZ observations planned in the *Planck* mission is discussed in [22].

Molecular rotational transitions could also be used to constrain the cosmological temperature-redshift law. So far, absorption and emission lines of CO, OH, CS, HCN,  $\text{HCO}^+$ ,  $\text{H}_2\text{O}$ ,  $\text{NH}_3$ , and other molecules have been observed in distant galaxies and quasars up to  $z = 6.42$  (for a recent review, see [23]). The absorption line observations are most suitable to the radiation temperature estimates since, as a rule, molecular absorption arise in the gas components with the lowest kinetic temperatures. A situation is to a large extent opposite to that of molecular emission from the warm gas clouds where excitation of the rotational levels is due to collisions with electrons. In the case of molecular absorption, the population of the lowest rotational levels is mainly caused by absorption of cosmic microwave background photons with only a minor possible contribution from collisions [18]. Up to now corresponding observations have been performed for two intermediate redshift systems: at  $z = 0.886$  toward the quasar PKS 1830-211 [24], and at  $z = 0.685$  toward the BL Lac object B0218+357 [25]. In the former case the unsaturated CS,  $\text{H}^{13}\text{CO}^+$ , and  $\text{N}_2\text{H}^+$  lines give the excitation temperature  $T_{\text{ex}} \approx 4 \pm 2$  K, whereas in the latter estimate the detected transitions  $J = 0 \rightarrow 1$  and  $J = 2 \rightarrow 3$  from CS yield  $T_{\text{ex}} \approx 6 (+3, -2)$  K. The  $\Lambda$ CDM model predict  $T(0.886) = 5.139 \pm 0.002$  K and  $T(0.685) = 4.592 \pm 0.002$  K. The relative error of these estimates ( $\delta \approx 50\%$ ) is much larger than the SZ values and therefore the concordance with the standard model is uncertain.

At higher redshifts ( $z > 1$ ), the CMB temperature can be evaluated from the analysis of quasar absorption line spectra which show atomic and/or ionic fine structure levels excited by the photo-absorption of the CMB radiation [26]. The most suitable are the fine structure levels of the ground states of CI ( $^3\text{P}_{0,1,2}$ ) and CII ( $^2\text{P}_{1/2,3/2}$ ) showing an energy separation between 24 K and 91 K. The CI lines were used in [27-30] to estimate the excitation temperature at, respectively,  $z = 1.776$  ( $T_{\text{ex}} = 7.4 \pm 0.8$  K),  $z = 1.973$  ( $T_{\text{ex}} = 7.9 \pm 1.0$  K),  $z = 2.338$  ( $T_{\text{ex}} = 10 \pm 4$  K), and  $z = 4.22413$  ( $T_{\text{ex}} = 14.93 \pm 0.87$  K). The first two values must be taken, however, with some caution since non-cosmological sources (such as particle collisions, pumping by the ambient UV radiation, and/or IR dust emission) may have contributed to the observed level populations. To estimate the contribution to the relative population of the fine-structure levels of the ground state of CI from competing excitation processes the independent analysis of the molecular hydrogen UV absorption lines may be of great

help. This approach was implemented in [29,30] where  $\text{H}_2$  transitions from different low rotational levels were used to infer the UV radiation field and the gas density in the CI- $\text{H}_2$  absorbers. In one high redshift system at  $z = 3.025$  [31] there were analyzed CII fine-structure transitions identified in the  $\text{H}_2$  bearing molecular cloud [32]. Utilizing constraints on the intensity of the UV and IR fields and on the volumetric gas density obtained from the analysis of populations of the  $J = 0-5$  rotational levels of  $\text{H}_2$ , dust density and metallicity, we calculated  $T_{\text{ex}} = 12.1(+1.7, -3.2)$  K. The expected  $\Lambda$ CDM value at this redshift is  $T(3.025) = 10.968 \pm 0.040$  K.

The estimates based on optical lines are still less certain than that obtained from the multifrequency SZ observations at lower redshifts [20,21]. The main problem here is systematic uncertainties caused by the unknown physical conditions in the absorbing clouds. To improve the accuracy of the CMB temperature measurement from absorption lines, higher resolution ( $FWHM \sim 1$  km/s) and signal-to-noise ( $S/N \sim 100$ ) spectra of QSOs are required in order to obtain more reliable physical parameters of the gas clouds.

Being combined, the results at low and high redshifts favour a linear scaling of the  $T(z)$  dependence (see Fig. 1). The parameter  $\beta$  from the modified relation  $T(z) = T(0)(1+z)^{1-\beta}$  is restricted at the  $1\sigma$  confidence level to  $\beta = -0.03 \pm 0.03$ . Thus, if the vacuum energy is decaying, its contribution to the CMB photons should be less than 6% ( $|\beta| < 0.06$ ) in the redshift range  $z \leq 4.2$ . It is to note that at the recombination epoch,  $z_{\text{rec}} \sim$

1100, the maximum value of  $\beta$  can be estimated from the fact that the density perturbations ( $\delta\rho/\rho$ ), as derived from the CMB and galaxy distribution data, do not differ by more than 10% [33]. This provides  $\beta_{\max} \approx 0.003$  under the assumption of a pressureless universe with an equation of state  $p/\rho \equiv w \equiv 0$ , where  $p$  is the pressure and  $\rho$  is the energy density [33]. At lower redshift, when  $w(z) < 0$  due to a vacuum energy contribution,  $\beta_{\max}$  may be different but its particular value should not exceed a few percents in accord with the observational constraints at  $z \leq 4.2$ . The influence of a decaying- $\Lambda$  term on the thermal evolution of the background radiation cannot be significant since otherwise it would lead to an earlier photon decoupling ( $z_{\text{rec}} \sim 2000$ ) which in turn would shift the CMB angular power spectrum to higher multipoles [15]. That the decay of the vacuum energy into CDM is ineffective was shown in [33]. The possibility of the decay into baryons has been ruled out earlier in [13] since the annihilation matter anti-matter (decay process does not violate baryon number) would produce a  $\gamma$ -ray background in excess of the observed level. Thus, if the vacuum energy is indeed decaying, it could decay either into hot dark matter (neutrinos as an example) or into exotic matter (e.g., scalar fields), since they do not affect the ( $\delta\rho/\rho$ ) and ( $\delta T/T$ ) CMB spectra [34]. The main problem with hot dark matter (HDM) models is, however, that they hamper the formation of small scale structures like galaxies. But as part of a mixed dark matter theory in which HDM supports large scale structure (clusters of galaxies) whereas CDM is responsible for smaller scales, HDM particles can be considered as possible products of the vacuum energy decay. The scalar fields as yet hypothetical fields in particle physics can be invoked to explain the accelerating Universe [35,36]. A consequence of this assumption is a dependence of coupling constants on cosmic time. The varying constants can, in turn, be used to infer the evolution of the scalar field, and thus to determine its equation of state [37]. Observational aspects of this cosmological test are considered in the next Section.

### 3. Constraints on variability of the fine-structure constant

A hypothetical variability of the fine-structure constant  $\alpha$ , widely discussed in the literature for the last few years and summarized in reviews [38,39], if real, could have a great impact on our understanding the main principles of nature. Recent result obtained in laboratory experiments with atomic clocks constrains the rate of the relative variation of  $\alpha$  as  $|d\alpha/dt/\alpha| < 4 \times 10^{-17} \text{ yr}^{-1}$  [40]. Comparable limits of  $1.8 \times 10^{-17} \text{ yr}^{-1}$  and  $7 \times 10^{-17} \text{ yr}^{-1}$  were set from the fission product analysis of a natural reactor in Oklo [41] and [42], respectively. The epoch of the Oklo phenomenon corresponds to the time interval of  $\Delta t \sim 2 \times 10^9 \text{ yr}$  ago ( $z \sim 0.14$ ). Being linearly extrapolated to higher redshifts ( $z > 1$ ,  $\Delta t \sim 10^{10} \text{ yr}$ ), these limits lead to  $|\Delta\alpha/\alpha| \equiv |(\alpha_z - \alpha)/\alpha| < 0.4 \text{ ppm}$  (ppm stands for parts per million,  $10^{-6}$ ). However, this extrapolation may not be valid for the values of  $\alpha$  at cosmic times. Contemporary theories predict very different patterns for  $\Delta\alpha/\alpha$  variations – from slow-rolling to oscillating [43-45]. Variations of  $\alpha$  at early cosmological epochs can be probed through the measurements of the relative radial velocity shifts between different metal absorption and molecular lines observed in quasar spectra. As was firstly shown in [46], different transitions in molecular hydrogen  $\text{H}_2$  have different sensitivities to variations of the proton to electron mass ratio,  $\mu = m_p/m_e$ . Later on, a many-multiplet (MM) method [47] was proposed to probe the variability of  $\alpha$  and sensitivity coefficients for many atomic and ionic transitions were calculated. The MM method was applied to metal absorption-line systems identified in Keck/HIRES and VLT/UVES spectra of several dozens of QSOs in [48-52].

The basic idea behind these publications was to estimate  $\Delta\alpha/\alpha$  using absorption lines of *different* elements (e.g., MgII, FeII, SiII, AlIII, etc.) and then to average over a large sample of the  $\Delta\alpha/\alpha$  values in order to cancel out random errors affecting the individual estimates. These individual estimates of  $\Delta\alpha/\alpha$  are of the order of 10-100 ppm, whereas the final  $\Delta\alpha/\alpha$  obtained from averaging over 143 absorption systems ranging between  $z = 0.2$  and  $z = 4.2$  is only  $\Delta\alpha/\alpha = -5.7 \pm 1.1 \text{ ppm}$  [50]. Such difference between the individual values and the resulting error of the mean  $\Delta\alpha/\alpha$  leads naturally to a certain concern with regard to the reliability of this error [53].

The result based on the 143 systems from the Keck QSO spectra was independently checked by the same MM method in [51], where 23 absorption systems identified in the VLT spectra of quasars and ranging between  $z = 0.4$  and  $z = 2.7$  were analyzed. After correcting for some certain computational shortcomings, it was obtained that  $\Delta\alpha/\alpha = 0.1 \pm 1.5 \text{ ppm}$  [54].

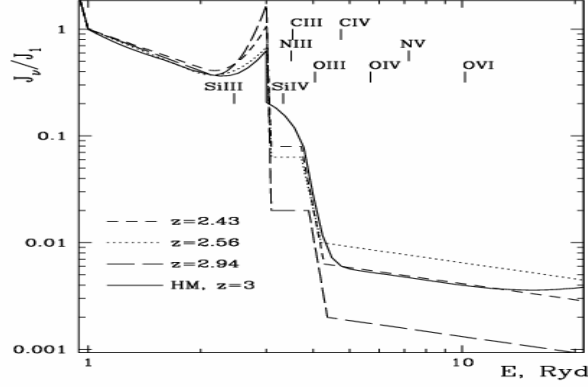


Fig. 2 The ionizing background spectra restored at different redshifts from optically thin metal absorbers [61]. The solid line is predicted for  $z = 3$  in [62]. The spectra are normalized so that  $J_\nu(h\nu = 1 \text{ Ryd}) \equiv 1$ . The emission bump at 3 Ryd is caused by reemission of HeII Ly $\alpha$ , HeII two-photon continuum emission and HeII Balmer continuum emission from intergalactic clouds. The positions of ionization thresholds of different ions observed in quasar absorption-line systems are indicated by tick marks. The continuum depression between 3 and 4 Ryd is due to HeII Ly $\alpha$  absorption in the IGM (the HeII Gunn-Peterson effect).

The variability of the product of two fundamental constants  $F = \alpha^2 \mu$  can be constrained from the [CII] 158  $\mu\text{m}$  line combined with CO rotational lines arising from the same molecular cloud. The most distant system of the [CII]-CO emission lines detected at  $z = 6.42$  in the spectrum of the quasar J1148+5251 ( $z = 6.42$ ) provides  $\Delta F/F = (0.1 \pm 1.0) \times 10^{-4}$  [69]. The corresponding look-back time is 93% of the total age of Universe.

It is clear that if  $\alpha$  is indeed oscillating then such behavior can be probed only by measurements at every particular  $z$ . To improve the accuracy of a single measurement we proposed a procedure referred to as the *Single Ion Differential  $\alpha$  Measurement* (SIDAM) described in detail in [55,56]. In this procedure  $\Delta\alpha/\alpha$  is measured from lines of only *one* ion – FeII, which makes the result free from the main uncertainty inherent to the MM method – namely, from random velocity shifts between *different* species caused by their non-cospatial origin. Moreover, the accuracy of the  $\Delta\alpha/\alpha$  measurement increases due to a larger difference between the sensitivity coefficients of FeII  $\lambda 1608$  and other FeII lines, and due to decreasing number of model parameters (all FeII lines arise from the same ground state level and, thus, have the same column density and broadening  $b$ -parameter, and trace the same volume elements). Using SIDAM and accounting for all known systematics including different correlation effects which were completely ignored in previous studies we obtained  $\Delta\alpha/\alpha = -0.12 \pm 1.79 \text{ ppm}$  at  $z = 1.15$ , and  $\Delta\alpha/\alpha = 4.4 \pm 3.5 \text{ ppm}$  at  $z = 1.84$  [57]. The latter value was derived from unique very high resolution spectra of the extremely bright quasar Q1101–264 ( $V = 16.0$ ,  $\text{FWHM} \cong 3.8 \text{ km s}^{-1}$ ,  $\text{S/N} \cong 100$  per pixel at the continuum level in the co-added spectrum) with calibration ThAr lamps taken immediately after scientific exposures. The former system at  $z = 1.15$  was re-observed with the high resolution pressure and temperature stabilized spectrograph HARPS mounted on the ESO 3.6m telescope at the La Silla observatory. It was obtained that  $\Delta\alpha/\alpha = 0.5 \pm 2.4 \text{ ppm}$  [58].

Another very stringent limit was recently placed on the proton to electron mass ratio from the comparison of the inversion transitions in  $\text{NH}_3$  with rotational spectra of CO,  $\text{HCO}^+$  and HCN observed in the absorption spectrum of the quasar B0218+357 at  $z = 0.68$  [39]:  $\Delta\mu/\mu = 0.6 \pm 1.9 \text{ ppm}$ . The error of this estimation does not account for the velocity offsets caused by possible non-cospatial distributions of molecules along the line of sight (so called the Doppler noise), but due to extremely high sensitivity of the  $\text{NH}_3$  inversion transitions to the change of  $\mu$ , the contribution from the Doppler noise will at maximum double the quoted error. Since most GUT models predict variation of  $\mu$  larger than that of  $\alpha$  [38], the obtained constraint on  $\Delta\mu/\mu$  leads to a conservative upper limit on  $|\Delta\alpha/\alpha| < 5 \text{ ppm}$  at  $z = 0.68$ . Thus, up to now several independent measurements carried out at different facilities agree in setting the limit on cosmological  $\alpha$  variations below the level of  $\sim 5 \text{ ppm}$ . Is it or will it be possible to access the level of 1 ppm ?

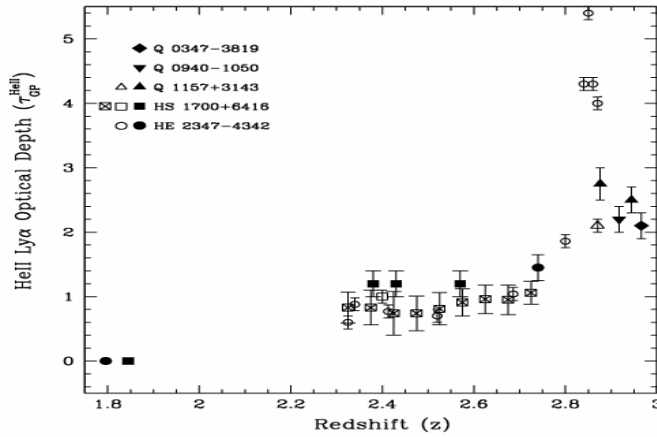


Fig. 3 Redshift dependence of the HeII Ly $\alpha$  opacity [61]. Open symbols show direct measurements from HE 2347-4342 [63], HS 1700+6416 (open square – [64], crossed open square – [65]), and Q 1157+3143 [66]. Filled symbols represent the opacities estimated from the restored spectral shapes of the metagalactic ionizing radiation field: diamond and reverse triangle [60], triangles, squares and circles [61]. Error bars correspond to  $1\sigma$  confidence level.

An uncertainty of 1 ppm corresponds to the error of the line position measurement less than  $30 \text{ m s}^{-1}$ . The requirement of such a high accuracy in observations of faint objects like QSOs is a challenging task even for the most powerful modern optical telescopes. However, new spectrographs such as the ESPRESSO (Echelle Spectrograph for PREcision Super Stable Observations), which is a high-efficiency, high-resolution, fiber-fed spectrograph of high mechanical and thermal stability, located at the incoherent Coude Focus of the VLT [59], are expected to provide a precision increase by at least one order of magnitude. Very promising appear to be differential measurements of the coupling constant on base of far infrared fine-structure lines [69,70], when the Stratospheric Observatory for Infrared Astronomy (SOFIA), the Herschel Space Observatory (HSO), and the Atacama Large Millimeter Array (ALMA) will go into operation in the nearest future. These forthcoming facilities will allow us to probe the variability of the fundamental physical constants with the accuracy higher than 1 ppm.

#### 4. Evolution of the spectral shape of the UV background with redshift

Spectral energy distribution of the intergalactic radiation in the far UV range is an important physical characteristic which governs many processes in the IGM. Metal lines observed in the intervening optically thin absorption systems can be used to recover the spectral shape of the metagalactic UV photoionizing background in the range  $E \sim 1\text{-}10 \text{ Ryd}$ . This range is defined by the ionization thresholds of ions observed in quasar absorbers (HI, CII-IV, OI-VI, SiII-IV, etc.). The corresponding computational procedure is described in [60]. The procedure was applied to the analysis of metal absorbers in the range  $1.6 < z < 2.9$  [60,61]. At  $2.4 \leq z \leq 2.9$ , the recovered spectral shapes show the intensity depression between 3 and 4 Ryd which is interpreted as a manifestation of the HeII Gunn-Peterson (GP) effect (Fig. 2). The values of the mean HeII Ly $\alpha$  opacity calculated from the depth of the GP trough correspond well to  $\tau_{\text{GP}}(\text{HeII})$  directly measured from the HI/HeII Ly $\alpha$  forest towards the quasars studied (Fig. 3). The background spectra reconstructed from the systems with  $z < 2$  are shown in Fig. 4. It is seen that the spectral shape of the UV background radiation fluctuates in the both redshift ranges studied. However, the fluctuations at  $z < 2$  and  $2.4 \leq z \leq 2.9$  are governed by different physical reasons. In the latter case, the fluctuations arise due to radiative transfer processes in the clumpy IGM, whereas at  $z < 2$  the IGM becomes almost transparent for both the HI and HeII Lyman continua and the variability of spectral shapes comes from diversity of spectral indices of the intrinsic QSO/AGN spectra.

The contribution to the metagalactic UV radiation field comes from two main sources: QSOs/AGNs and galaxies. The recovered spectra show unambiguously that at  $z < 3$  the UV background is produced mostly by QSO/AGN radiation processed by the clumpy IGM. No traces of the input of radiation from soft sources like starburst galaxies are revealed. Thus, only a very small soft spectrum component from star-

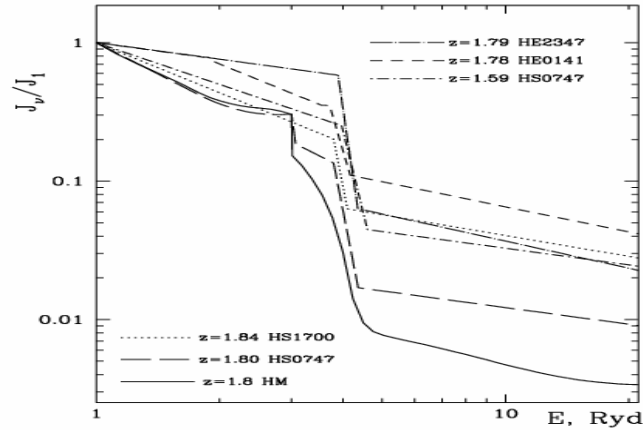


Fig. 4 The difference between the spectral shape of the UV background predicted at  $z = 1.8$  in [62] (solid line) and those restored from optically thin metal absorbers. The data are taken from: [61] - quasars HE 2347-4342 and HS 1700+6416; [67] - HE 0141-3932; and [68] - HS 0747+4259.

forming regions may contribute to the metagalactic ionizing radiation field, suggesting that an escape fraction of the ionizing photons with energy  $E > 1$  Ryd is  $f_{\text{esc}} < 5\%$ .

## References

1. Osterbrock D.E., Ferland G.J. *Astrophysics of Gaseous Nebulae and Active Galactic Nuclei* / University Science Books, Sansalito, CA, 2006.
2. Fan X., Strauss M.A., Becker R.H. et al. // *AJ*. 132, 117 (2006).
3. D'Odorico V. // *A&A*. 470, 523 (2007).
4. Quast R., Reimers D., Baade R. // *A&A*. 477, 443 (2008).
5. Levshakov S.A., Varshalovich D.A. // *MNRAS*. 212, 517 (1985).
6. Ledoux C., Petitjean P., Srianand R. // *ApJ*. 640, L25 (2006).
7. Meiksin A.A. // *Rev. Mod. Phys.* in press, arXiv: 0711.3358 (2008).
8. Perlmutter S. et al. // *ApJ*. 517, 565 (1999).
9. Riess A.G., Stolger L.-G., Casertano, S. et al. // *ApJ*. 659, 98 (2007).
10. Komatsu, E., Dunkley J., Nolte M.R. et al. // *ApJS*, submit., arXiv: 0803.0547 (2008).
11. Weinberg S. // *Rev. Mod. Phys.* 61, 1 (1989).
12. Sahni V., Starobinsky A. // *Int. J. Mod. Phys. D*. 50, 4890 (2000).
13. Freese K., Adams F.C., Frieman J.A., Mottola E. // *Nucl. Phys. B*. 287, 797 (1987).
14. Puy D. // *A&A*. 422, 1 (2004).
15. Nakamura R., Hashimoto M., Ichiki K. // *Phys. Rev. D*. submit., arXiv: 0801.0290 (2008).
16. Lima J.A.S., Silva A.I., Viegas S.M. // *MNRAS*. 312, 747 (2000).
17. Mather J.C., Fixsen D.J., Shafer R.A. et al. // *ApJ*. 512, 511 (1999).
18. Roth K.C., Meyer D.M. // *ApJ*. 441, 129 (1995).
19. Welty D.E., Federman S.R., Gredel R. et al. // *ApJS*. 165, 138 (2006).
20. Battistelli E.S., De Petris M., Lamagna L. et al. // *ApJ*. 580, L101 (2002).
21. Battistelli E.S., De Petris M., Lamagna L. et al. // *Mem. S. A. It.* 74, 316 (2003).
22. Horellou C., Nord M., Johansson D., Levy A. // *A&A*. 441, 435 (2005).
23. Omont A. // *Rep. Prog. Phys.* 70, 1099 (2007).
24. Wiklind T., Combes F. // *Nature*. 379, 139 (1996).
25. Combes F., Wiklind T., Nakai N. // *A&A*. 327, L17 (1997).
26. Bahcall J.N., Wolf R.A. // *ApJ*. 152, 701 (1968).
27. Songaila A., Cowie L.L., Vogt S. et al. // *Nature*. 371, 43 (1994).
28. Ge J., Bechtold J., Black J.H. // *ApJ*. 474, 67 (1997).
29. Srianand R., Petitjean P., Ledoux C. // *Nature*. 408, 931 (2000).
30. Ledoux C., Petitjean P., Srianand R. // *ApJ*. 640, L25 (2006).
31. Molaro P., Levshakov S.A., Dessauges-Zavadsky M., D'Odorico S. // *A&A*. 381, L64 (2002).
32. Levshakov S.A., Dessauges-Zavadsky M., D'Odorico S., Molaro P. // *ApJ*. 565, 696 (2002).
33. Opher R., Pelinson A. // *MNRAS*. 362, 1670 (2005).
34. Opher R., Pelinson A. // *BrJPh*. 35, 1206 (2005).
35. Peebles P.J.E., Ratra B. // *Rev. Mod. Phys.* 75, 559 (2003).
36. Copeland E.J., Sami M., Tsujikawa S. // *Int. J. Mod. Phys. D*. 15, 1753 (2006).
37. Avelino P.P., Martins C.J.A.P., Nunes N.J., Olive K.A. // *Phys. Rev. D*. 74, 083508 (2006).
38. Flambaum V.V. // arXiv: nucl-th/0801.1994 (2008).

39. Flambaum V.V., Kozlov M.G. // arXiv: physics.atom-ph/0711.4536 (2008).
40. Rosenband T., Hume D.B., Schmidt P.O. et al. // Scienceexpress. 6 March (2008).
41. Gould C.R., Sharapov E.I., Lamoreaux S.K. // Phys. Rev. C. 74, 024607 (2006).
42. Petrov Yu.V., Nazarov A.I., Onegin M.S. et al. // Phys. rev. C. 74, 064610 (2006).
43. Marciano W.J. // Phys. Rev. Lett. 52, 489 (1984).
44. Mota D.F., Barrow J.D. // MNRAS. 349, 291 (2004).
45. Fujii Y. // Phys. Lett. B. 616, 141 (2005).
46. Varshalovich D.A., Levshakov S.A. // JETP Lett. 58, 237 (1993).
47. Dzuba V.A., Flambaum V.V., Webb J.K. // Phys. Rev. A. 59, 230 (1999).
48. Webb J.K., Flambaum V.V., Churchill C.W. et al. // Phys. Rev. Lett. 82, 884 (1999).
49. Murphy M.T., Webb J.K., Flambaum V.V. // MNRAS, 345, 609 (2003).
50. Murphy M.T., Flambaum V.V., Webb J.K. et al. / Astrophysics, Clocks and Fundamental Constants, eds. S.G. Karshenboim and E. Peik / Berlin, Springer-Verlag, 2004, p.131.
51. Chand H., Srianand R., Petitjean P., Aracil B. // A&A. 417, 853 (2004).
52. Murphy M.T., Webb J.K., Flambaum V.V. // MNRAS. in press, arXiv: astro-ph/0612407 (2008).
53. Bahcall J.N., Steinhart C.L., Schlegel D. // ApJ. 600, 520 (2004).
54. Srianand R., Chand H., Petitjean P., Aracil B. // Phys. Rev. Lett. 100, 029902 (2008).
55. Levshakov S.A. / Astrophysics, Clocks and Fundamental Constants, eds. S.G. Karshenboim and E. Peik / Berlin, Springer-Verlag, 2004, p.151.
56. Levshakov S.A., Centurion M., Molaro P., D'Odorico S. // A&A. 434, 827 (2005).
57. Levshakov S.A., Agafonova I.I., Molaro P., Reimers D. // A&A. submit. (2008).
58. Chand H., Srianand R., Petitjean P. et al. // A&A. 451, 45 (2006).
59. Molaro P. // arXiv: astro-ph/0712.4390 (2008).
60. Agafonova I.I., Centurion M., Levshakov S.A., Molaro P. // A&A. 441, 9 (2005).
61. Agafonova I.I., Levshakov S.A., Reimers D. et al. // A&A. 461, 893 (2007).
62. Haardt F., Madau P. // ApJ. 461, 20 (1996).
63. Zheng W., Kriss G.A., Deharveng J.-M. et al. // ApJ. 605, 631 (2004).
64. Davidsen A., Kriss G.A., Zheng W. // Nature. 380, 47 (1996).
65. Fechner C., Reimers D., Kriss G.A. et al. // A&A. 455, 91 (2006).
66. Reimers D., Fechner C., Hagen H.-J. et al. // A&A. 442, 63 (2005).
67. Reimers D., Janknecht E., Fechner C. et al. // A&A. 435, 17 (2005).
68. Reimers D., Agafonova I.I., Levshakov S.A. et al. // A&A. 449, 9 (2006).
69. Levshakov S.A., Reimers D., Kozlov M.G. et al. // A&A. 479, 719 (2008).
70. Kozlov M.G., Porsev S.G., Levshakov S.A. et al. // Phys. Rev. A. in press, arXiv: physics.atom-ph/0802.0269 (2008).